Dynamic Multiobjective Approach for Power and Spectrum Allocation in Cognitive Radio Networks

Chih-Lin Chuang, Wei-Yu Chiu, *Member, IEEE*, and Yu-Chieh Chuang

***Abstract*—Cognitive radio (CR) is a promising technology for addressing resource scarcity in wireless networks. However, in the current CR-based framework, when resource availability changes, existing resource allocation algorithms restart the optimization process without using historical information. In addition, most previous studies have focused on one or two objectives and some have only addressed pure power control or spectrum allocation, limiting the potential of CR. Thus, this article proposes a dynamic multiobjective approach for power and spectrum allocation in a CR-based environment in which the available spectrum channels vary over time and multiple objectives are involved. This article presents a dynamic multiobjective optimization problem (MOP) with the objectives of energy efficiency, fairness, and spectrum utilization and an approach of Pareto optimality. A dynamic resource allocation algorithm comprising a hybrid initialization method and feasible point generation mechanisms is proposed to solve the dynamic MOP. To dynamically adjust resource allocation, historical approximate Pareto optimal solutions, represented by a center and a manifold, are used to predict the new optima. The proposed approach can yield a better convergence level and convergence rate than those attained by comparable multiobjective resource allocation algorithms. Compared with conventional single-objective approaches, it achieves an excellent balance between the objectives.**

***Index Terms*—Cognitive radio (CR), dynamic multiobjective optimization, energy efficiency, fairness, resource allocation, spectrum utilization.**

I. Introduction

With the Internet of Things emerging in global networks of machines, devices, and everyday objects, more data must be transmitted wirelessly [1]–[3]; this, in turn, has significantly increased the demands on spectrum bands and power in wireless networks. Cognitive radio (CR) is a promising technology that can address the problems of spectrum scarcity and the inefficient use of the spectrum [4], [5]. Users in CR networks can be classified as primary or secondary depending on whether they use licensed or unlicensed spectrum bands, respectively. CR technology senses the idle spectrum bands (called spectrum holes) of the primary users and then allows the secondary users to use these bands [6]–[8].

Manuscript received May 13, 2020; revised October 30, 2020 and January 20, 2021; accepted February 19, 2021. Date of publication March 25, 2021; date of current version December 9, 2021. This work was supported by the Ministry of Science and Technology of Taiwan under Grant MOST 109-2221-E-007-020. *(Corresponding author: Wei-Yu Chiu.)*

The authors are with the MOCaRL Lab, Department of Electrical Engineering, National Tsing Hua University, Hsinchu 300044, Taiwan (e-mail: kenny655021@gmail.com; chiuweiyu@gmail.com; jack3168@gmail.com).

Digital Object Identifier 10.1109/JSYST.2021.3061670

CR can be divided into two phases. The first phase involves sensing spectrum holes (i.e., sensing idle channels), and various methods have been proposed for this purpose. For example, hidden Markov models are used to predict the idle channels on the basis of the previous channel states [9], [10] and neural networks have been developed to reduce dependence on prior knowledge regarding network traffic characteristics [11]. The second phase involves resource allocation, where power or spectrum bands, or both, are allocated.

In this article, we used some previously proposed prediction methods and primarily focused on a resource allocation problem in a CR network. While addressing this problem, we considered its size to be proportional to the numbers of users and spectrum channels [12]–[15]. To reduce the problem size, some studies have assumed that all users share the same spectrum channel, for which only power control is considered [16]–[18]. However, owing to the interference between users, the spectrum channel cannot sufficiently support the massive data transmission on the entire network. Some other studies have assumed that each user transmits at a fixed power or data rate. However, in assuming so, these studies have only addressed spectrum allocation [19]–[21], which may result in power wastage during the data transmission. Therefore, to realize the complete potential of a CR network, it is reasonable to consider the joint allocation of power and spectra.

Resource allocation in a CR network aims to achieve energy efficiency, spectrum utilization, and fairness. Energy efficiency measures how efficiently power is consumed for data transmission [15], [17], [18], [22], [23]; spectrum utilization evaluates how limited spectrum channels can be used for spectrum assignment [12], [23], [24]; and fairness assesses how fairly the resources of a CR network are shared by users [25]. To achieve these aims, a single-objective optimization problem considering at most two of those metrics as objectives for resource allocation has already been formulated. In [26] and [27], for example, energy efficiency in beamforming for a coordinated multicell multiuser downlink system was examined. In [28] and [29], a framework addressing energy efficiency and spectrum utilization in massive MIMO-enabled HetNets was proposed. In terms of fairness, a max–min fairness metric was used to ensure that the worst performance of a user is repaired and maximized, a proportional fairness metric was used to allocate resources in proportion with user demand, and Jain's fairness metric was used to ensure that each user delivers the same performance [16], [21], [30].

In practice, however, the aforementioned metrics can have conflicting objectives. For instance, when spectrum utilization is

improved, the number of idle channels decreases, causing much interference because of the presence of more secondary users sharing a limited number of channels. As the interference increases, the signal-to-interference-plus-noise ratio (SINR) may decrease, which further undermines the energy efficiency. By contrast, better energy efficiency can be achieved by allocating more resources to secondary users, who possess better channels; however, this jeopardizes user fairness. Because of these conflicting objectives, single-objective optimization cannot efficiently balance between these metrics [31].

To address this issue, a multiobjective optimization problem (MOP) has been proposed, and Pareto optimality has been adopted [13], [19], [32]. For example, Bhardwaj *et al.* [13] proposed a multiband CR network scenario under quality-of-service constraints, and they applied a modified nondominated sorting genetic algorithm II (NSGA-II) algorithm to obtain approximate Pareto optimal solutions. Han *et al.* [19] proposed an NSGA-II-based algorithm to optimize end-to-end throughput and spectrum utilization. Anumandla *et al.* [32] proposed a multiobjective differential evolution-based algorithm to address spectrum utilization, max–min fairness, and proportional fairness.

However, two major factors can render the evolution process inefficient. First, these multiobjective evolutionary algorithms for resource allocation only consider a static environment in which the number of idle spectra is fixed; when resource availability changes, the allocation algorithms restart the optimization process without using the available historical information. Second, efficient techniques for handling physical constraints imposed on CR networks have not been comprehensively investigated. For example, a tree pruning method [13] was used to directly remove infeasible points from the population, ignoring the fact that some infeasible points are close to the feasible points. Generic penalty methods can be adopted to better use the information extracted from infeasible points; however, these methods might yield premature or overdue convergence problems [33].

Although dynamic resource allocation in CR networks has not been comprehensively investigated, the concept of dynamically tracking new optima has been explored in the literature on evolutionary computation [34]. Zhou *et al.* [35] investigated a population prediction strategy for dynamic evolutionary multiobjective optimization. In this method, the points in a Pareto set were either represented as a center point or a manifold; an autoregression model and the Euclidean distance were used to predict the center point and manifold as they evolve through time, respectively. Populations were then initialized using the information on historical solutions. Xu *et al.* [36] developed a cooperative coevolution strategy based on environmental sensitivities. They adopted the differential prediction and Cauchy mutation strategies for determining the decision variables on the basis of their interrelation with the environment.

Motivated by the concept of dynamically tracking Pareto optimal solutions, in this article, we address the problem of resource allocation in a CR network by considering a dynamic MOP with the objectives of energy efficiency, fairness, and spectrum utilization. In the proposed problem, spectrum allocation and power control are considered the discrete and continuous decision variables to be determined, respectively, and the number of idle spectra is considered to vary dynamically with time. To address this dynamic MOP, we propose a dynamic multiobjective resource allocation algorithm, which comprises a hybrid initialization method and feasible point generation mechanisms. The hybrid initialization method can dynamically track the new optima based on historical approximate Pareto optimal sets. The mechanisms of generating feasible points can avoid the need to use penalty methods for constraint handling. As such, the resulting algorithm may exhibit improved efficiency and be less affected by premature or overdue convergence problems. Solving the dynamic MOP yields an approximate Pareto optimal set and a Pareto front. The resources among secondary users in a CR network are allocated on the basis of a Pareto optimal solution. The simulation results indicate that the proposed methodology can efficiently achieve an excellent balance between the objectives relative to the existing methods.

This article makes the following three contributions to the literature. First, our problem formulation has not been investigated in conventional CR networks; most previous studies have focused on one or two of these objectives, and some have only considered one type of our decision variables (i.e., discrete or continuous). The scenario considered in this article is more challenging and the network flexibility induced by this scenario can be helpful in realizing the complete potential of CR systems. Second, we develop a few mechanisms that can search for feasible points more efficiently than the conventional penalty methods can, yielding a better convergence rate and level than those attained by comparable evolutionary algorithms. Third, the proposed multiobjective approach can dynamically track a new Pareto optimal allocation, whereas the existing resource allocation algorithms for CR networks must restart the optimization whenever the network environment changes.

The rest of this article is organized as follows. Section II describes the system models involved in a CR network, including the metrics of energy efficiency, fairness, and spectrum utilization. In Section III, our dynamic multiobjective approach is detailed and analyzed. Section IV presents the simulation results involving performance comparisons in terms of the convergence rate, convergence level, and objective values. Finally, Section V concludes this article.

II. System Models

This section presents the system model that describes the spectrum allocation and power control schemes in the CR network. In each period t, the primary users may lease a few licensed spectrum channels under certain interference conditions. Meanwhile, the secondary users submit their communication demand for them to be assigned a certain amount of power and a certain number of spectrum channels [37]–[39].

Table I summarizes the notation used throughout this article. A CR network can be considered a multihop network, and one node in the network can use the other nodes as relays to reach

TABLE I
NOTATION

t	Time slot
$\mathcal{N}$	Set of nodes
$\mathcal{L}$	Set of links
(i,j)	Link comprising sender i and receiver j where $(i,j) \in \mathcal{L}$ and $\forall i,j \in \mathcal{N}$
$\mathcal{F}$	Set of data flows between sources and destinations
f	Data flow
$\mathcal{M}(t)$	Set of available spectrum channels at time t
$c_{(i,j)}(t)$	Spectrum channel assigned to (i,j) at time t where $c_{(i,j)}(t) \in \mathcal{M}(t)$
$P_{(i,j)}(t)$	Power consumed by link (i,j) at time t
$P^{\min}$	Minimum power consumption of (i,j)
$P^{\max}$	Maximum power consumption of (i,j)
$\mathcal{L}_i$	Set of links sharing node i
$\mathcal{L}_{c_{(i,j)}(t)}$	Set of links sharing $c_{(i,j)}(t)$
$\mathcal{L}^f$	Set of links that constitute f
$l_{i,j}$	Path loss between node i and node j
$\text{SINR}_{(i,j)}(t)$	Signal-to-interference-plus-noise ratio of (i,j) at time t
$q_{(i,j)}$	Transmission opportunity of (i,j)
$R_{(i,j)}(t)$	Data rates of (i,j) at time t
$\mathcal{M}_u(t)$	Set of spectrum channels occupied by $\mathcal{L}$ at time t

its destination. Let $\mathcal{N}$ be a set of nodes. A link comprising a pair of nodes allows data to be transmitted between the nodes. Let $\mathcal{L}$ denote a set of links and (i,j) denote a link comprising a sender i and receiver j, where $(i,j) \in \mathcal{L}$ and $\forall i,j \in \mathcal{N}$. Let $\mathcal{F}$ denote a set of data flows, each of which represents a routing path comprising links between a source and destination in the network.

In this scheme, the number of available channels for supporting data transmission fluctuates over time. In general, the occupied and idle channels can be modeled as a stationary exponential random process [20]. The ON or OFF states indicate whether the spectrum channel is occupied by primary users or is idle, respectively. The ON and OFF stationary probabilities, Pr^{ON} and Pr^{OFF}, of an idle spectrum channel can be expressed as

$$\text{Pr}^{\text{ON}} = \frac{\mu}{\lambda+\mu} \quad \text{Pr}^{\text{OFF}} = \frac{\lambda}{\lambda+\mu} \tag{1}$$

where μ and λ represent the occupied and idle transition rates of the spectrum channel, respectively.

For data transmission, each link is assigned a spectrum channel and certain amount of power. Fig. 1 illustrates a resource allocation scheme [19]. Let $\mathcal{M}(t)$ denote a set of idle channels and $c_{(i,j)}(t)$ denote the spectrum channel assigned to link (i,j) at time t, which satisfies the following condition:

$$c_{(i,j)}(t) \in \mathcal{M}(t). \tag{2}$$

Let $P_{(i,j)}(t)$ denote the power consumed by link (i,j) at time t, which satisfies

$$P^{\min} \le P_{(i,j)}(t) \le P^{\max} \tag{3}$$

where $P^{\min}$ and $P^{\max}$ indicate the minimum and maximum power consumed by link (i,j), respectively.

Data transmission in a communication network can be affected by factors, such as fading and SINR. Three types of fading are widely considered: path loss; slow fading, caused by shadowing; and fast fading, caused by the Doppler effect

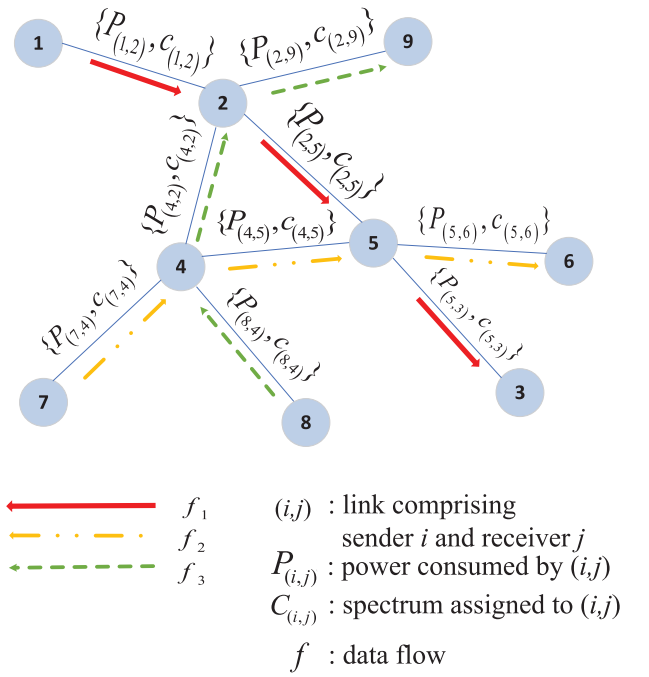

Fig. 1. Illustration of power control and spectrum allocation in a CR network.

and multipath delay. This article assumes that path loss as the dominating fading effect [13], [40]; the path loss function can be expressed as

$$l_{i,j} = \frac{G_i^{\text{Tx}} G_j^{\text{Rx}}}{d_{i,j}^{\alpha}} \tag{4}$$

where G_i^{Tx} and G_j^{Rx} represent the antenna gains of transmitter i and receiver j, respectively; $d_{i,j}$ is the distance between nodes i and j; and α is the loss exponent parameter. The SINR at time t can be expressed as [13]

$$\text{SINR}_{(i,j)}(t) = \frac{l_{i,j} P_{(i,j)}(t)}{\epsilon_0 + \sum_{(a,b) \in \mathcal{L}_{c_{(i,j)}(t)} \setminus \{(i,j)\}} l_{a,j} P_{(a,b)}(t)} \tag{5}$$

where $\epsilon_0 \sim N(0, \sigma_0^2)$ is a Gaussian random variable with a mean of 0 and variance of σ_0^2 and $\mathcal{L}_{c_{(i,j)}(t)}$ is a set of links sharing the spectrum channel $c_{(i,j)}(t)$. A constraint on (5) is imposed as

$$\text{SINR}_{(i,j)}(t) \ge \gamma \tag{6}$$

where γ represents an SINR threshold.

In the CR network, each node has only one transceiver, which cannot transmit and receive data simultaneously. Therefore, the maximum capacity of each node is equally distributed to the links [19]. Let the set of links sharing node i be denoted as

$$\mathcal{L}_i = \{(a,b) |\ a = i \ \vee \ b = i,\ (a,b) \in \mathcal{L}\}. \tag{7}$$

Then, the transmission opportunity on link (i,j) is expressed as

$$q_{(i,j)} = \min\left\{ \left| \frac{1}{\mathcal{L}_i} \right|, \left| \frac{1}{\mathcal{L}_j} \right| \right\} \quad \forall i,j \in \mathcal{N}. \tag{8}$$

The data rates of link (i, j) at time t can then be expressed in terms of (5) and (8), as follows:

$$R_{(i,j)}(t) = q_{(i,j)} B \log_2(1 + \text{SINR}_{(i,j)}(t)) \tag{9}$$

where B is the bandwidth of the spectrum channel.

The variables $c_{(i,j)}(t)$ and $P_{(i,j)}(t)$ are controlled to achieve optimal transmission performance. For simplicity in the following discussion, we introduce the following notation:

$$\boldsymbol{x}(t) = \left[\cdots \; c_{(i,j)}(t) \; \cdots \; P_{(i,j)}(t) \; \cdots \right] \tag{10}$$

where $\boldsymbol{x}(t)$ comprises $2|\mathcal{L}|$ decision variables—specifically, $|\mathcal{L}|$ discrete decision variables $c_{(i,j)}(t)$ and $|\mathcal{L}|$ continuous decision variables $P_{(i,j)}(t)$. To appropriately distribute the power and spectrum channels among secondary users, we consider the following performance metrics: energy efficiency, fairness, and spectrum utilization.

Energy efficiency can be defined as the ratio of the network throughput to power consumption [41]

$$F_{\text{EE}}(\boldsymbol{x}(t)) = \frac{\sum_{f \in \mathcal{F}} \sum_{(i,j) \in \mathcal{L}^f} R_{(i,j)}(t)}{\sum_{f \in \mathcal{F}} \sum_{(i,j) \in \mathcal{L}^f} P_{(i,j)}(t)} \tag{11}$$

where $\mathcal{L}^f$ is the set of links that constitute the data flow f.

According to (4), the SINR expressed in (5) decreases with the distance between two nodes. The data rates may fluctuate greatly between the links in each data flow. Thus, fairness can be expressed as follows [13]:

$$F_{\text{Fair}}(\boldsymbol{x}(t)) = \sum_{f \in \mathcal{F}} \sum_{(i,j) \in \mathcal{L}^f} (R_{(i,j)}(t) - \bar{R}(t))^2 \tag{12}$$

where

$$\bar{R}(t) = \frac{1}{|\mathcal{L}^f|} \sum_{(i,j) \in \mathcal{L}^f} R_{(i,j)}(t).$$

For the full utilization of the spectrum channels for data transmission, spectrum utilization is considered and defined as follows [19]:

$$F_{\text{Spec}}(\boldsymbol{x}(t)) = \frac{|\mathcal{L}|}{|\mathcal{M}_u(t)|} \tag{13}$$

where $\mathcal{M}_u(t)$ is the set of spectrum channels occupied by $\mathcal{L}$ at time t. For instance, let $\mathcal{M}(t) = \{m_1, m_2, m_3\}$, where m_1 and m_3 are assigned to the links for data transmission; we have $\mathcal{M}_u(t) = \{m_1, m_3\}$.

III. Proposed Dynamic Multiobjective Approach

This section presents a dynamic multiobjective approach for resource allocation among secondary users in a CR network. A dynamic MOP that considers energy efficiency expressed in (11), fairness expressed in (12), and spectrum utilization expressed in (13) is formulated. To efficiently explore the decision variable space, we developed a few methods for generating feasible values for the two types of decision variables; we then analyze these methods for feasibility. Subsequently, a dynamic multiobjective evolutionary algorithm is proposed to approximate the Pareto optimal solutions.

The dynamic MOP is formulated as

$$\begin{aligned} &\max_{\boldsymbol{x}(t)} F_{\text{EE}}(\boldsymbol{x}(t)) \\ &\min_{\boldsymbol{x}(t)} F_{\text{Fair}}(\boldsymbol{x}(t)) \\ &\max_{\boldsymbol{x}(t)} F_{\text{Spec}}(\boldsymbol{x}(t)) \\ &\text{subject to } (2), (3), \text{ and } (6) \end{aligned} \tag{14}$$

where $F_{\text{EE}}(\boldsymbol{x}(t))$ and $F_{\text{Fair}}(\boldsymbol{x}(t))$ are conflicting objective functions. Maximizing the energy efficiency $F_{\text{EE}}(\boldsymbol{x}(t))$ can lead to allocating more resources to users with better channels, thus degrading user fairness (i.e., yielding a large value of $F_{\text{Fair}}(\boldsymbol{x}(t))$). $F_{\text{Spec}}(\boldsymbol{x}(t))$ and $F_{\text{EE}}(\boldsymbol{x}(t))$ are also conflicting objective functions. Increasing the spectrum utilization $F_{\text{Spec}}(\boldsymbol{x}(t))$ deceases the number of idle channels, causing much interference and reducing the SINR; a smaller SINR value implies less energy efficiency as measured by $F_{\text{EE}}(\boldsymbol{x}(t))$. Given such a conflict, a global optimal solution that simultaneously achieves these objectives does not exist, and hence, conventional and efficient single-objective optimization algorithms cannot be applied in this case. As such, a Pareto optimality approach [42] must be adopted, which induces much complexity.

Remark 1: A Pareto optimal (also called nondominated) solution indicates the impossibility of improving one objective value without degrading the others. Thus, a set of approximate Pareto optimal solutions is desired, which can be obtained by solving the dynamic MOP. The associated objective vectors of the approximate Pareto set are termed as the approximate Pareto front.

In addition to the complexity induced by the conflicting objectives, the following two types of decision variables are involved in (14): 1) discrete spectrum allocation variables $c_{(i,j)}(t)$ and 2) continuous power control variables $P_{(i,j)}(t)$ in $\boldsymbol{x}(t)$. Although conventional population-based multiobjective evolutionary algorithms can be used to determine an approximate Pareto set of MOPs [43], they usually consider purely continuous or discrete decision variables. An MOP with mixed types of decision variables, such as those indicated in (14), has not been thoroughly investigated in the literature.

Another layer of difficulty in solving (14) originates from the constraint expressed in (6), which introduces nonbox constraints on the decision variables. Box constraints, such as those shown in (3), can be readily addressed within the framework of generic evolutionary algorithms, whereas nonbox constraints, such as those expressed in (6), require a special mechanism during the evolution process. Algorithms can use penalty methods to address nonbox constraints; however, this technique cannot efficiently determine the feasible points.

Remark 2: In a penalty method for addressing maximization problems, a penalty is subtracted from the objective functions if a point violates the constraints; infeasible points are then eliminated gradually during the evolution process. In this case, a scaling constant is required to indicate how great a penalty to levy for the violation; a bad choice of the constant may lead to premature or overdue convergence. Furthermore, there

is no guarantee on how fast the penalty method can remove the infeasible points from the population; if the removal is slow, the algorithm has low efficiency.

Finally, problem (14) has a dynamic property, as indicated by the presence of the temporal term t. The number of idle channels can vary with time. As such, population initialization in multiobjective evolutionary algorithms is often required when the environment associated with the problem changes, which further decreases the algorithm's efficiency during the observation period. To address the difficulties induced by multiple conflicting objectives, mixed types of decision variables, nonbox constraints, and the dynamic property, feasible search mechanisms, and efficient initialization for mixed types of decision variables and multiple objectives are required.

As a first step to developing these methods, we consider the following generic procedure of multiobjective evolutionary algorithms. First, an initial population that comprises points is randomly generated. Second, genetic operations, such as crossover and mutation, are applied to generate a new population. In this step, crossover is performed on a pair of candidate points and produces another pair of points, termed as the offspring; in addition, mutation is performed on a candidate point and produces a new point, termed as a mutant. Genetic operations are often conducted probabilistically. Third, a few points are selected from the original and new populations on the basis of their associated performance, and points are removed if they exhibit low Pareto optimality. This evolution process is iterated until a certain stopping criterion is attained.

Following the aforementioned generic procedure, we propose Algorithm 1 to efficiently initialize the points during the observation period. Then, genetic operations involving crossover and mutation are applied to the points in accordance with Algorithms 2 and 3, respectively, during the evolution process. If the points are infeasible, they are repaired using Algorithm 4. Finally, using Algorithms 1–4, Algorithm 5 produces an approximate Pareto set and front, and selects a final solution for power and spectrum allocation in the CR network.

For population initialization, Algorithm 1 adopts a prediction strategy modified from [35] to track the new optima. Let T denote the memory size of the database that stores previous data points. We first construct the database if the historical information is insufficient to construct a prediction model. The following notations are used to represent point $\boldsymbol{x}_n(t)$ in the population $\Gamma(t)$ and the components $c_{n,(i,j)}(t)$ and $P_{n,(i,j)}(t)$ of this point:

$$\Gamma(t) = \{\boldsymbol{x}_1(t), \boldsymbol{x}_2(t), \ldots, \boldsymbol{x}_{N_{\max}}(t)\} \tag{15}$$

where

$$\boldsymbol{x}_n(t) = \left[\cdots\ c_{n,(i,j)}(t)\ \cdots\ P_{n,(i,j)}(t)\ \cdots\right],\quad n = 1, \ldots, N_{\max}.$$

Owing to the dynamic feature of the available resources, the boundary of the discrete decision variables varies over time and makes dynamic optimization more difficult. To address this issue, in Step 1.1 of Algorithm 1, let us transform the discrete decision variables into continuous variables within a fixed interval (i.e., $c_{n,(i,j)}(t-\rho) \in (0,1], \rho = 1, 2, \ldots, \min\{t-1, T\}$). In Steps 1.2 and 1.3, each component of the point is represented by a center and a manifold. In Step 1.2, an autoregression model is applied to predict the centers $\bar{c}_{n,(i,j)}(t)$ and $\bar{P}_{n,(i,j)}(t)$, which can be described as

$$\begin{aligned}\bar{c}_{n,(i,j)}(t) &= \sum_{\tau=1}^{g} \lambda_{n,\tau,c}\bar{c}_{(i,j)}(t-\tau) + \epsilon_{n,(i,j),\bar{c}} \\ \bar{P}_{n,(i,j)}(t) &= \sum_{\tau=1}^{g} \lambda_{n,\tau,p}\bar{P}_{(i,j)}(t-\tau) + \epsilon_{n,(i,j),\bar{p}}\end{aligned} \tag{16}$$

where $\epsilon_{n,(i,j),\bar{c}} \sim N(0, \sigma^2_{n,(i,j),\bar{c}})$, $\epsilon_{n,(i,j),\bar{p}} \sim N(0, \sigma^2_{n,(i,j),\bar{p}})$, $\lambda_{n,\tau,c}$ and $\lambda_{n,\tau,p}$ denote the autoregression parameters, and $\bar{c}_{(i,j)}(t-\tau)$ and $\bar{P}_{(i,j)}(t-\tau)$ are calculated as

$$\begin{aligned}\bar{c}_{(i,j)}(t-\tau) &= \frac{1}{N_{\max}} \sum_{n=1}^{N_{\max}} c_{n,(i,j)}(t-\tau) \\ \bar{P}_{(i,j)}(t-\tau) &= \frac{1}{N_{\max}} \sum_{n=1}^{N_{\max}} P_{n,(i,j)}(t-\tau).\end{aligned}$$

Remark 3: In (16), the centers of interest, $\bar{c}_{n,(i,j)}(t)$ and $\bar{P}_{n,(i,j)}(t)$, are predicted using a linear combination of historical data to which white noise is added. This prediction method is based on the assumption that the underlying network dynamics change gradually with time. As such, the current Pareto optimal solutions of interest are close to the past Pareto optimal solutions; thus, the added white noise provides perturbations to the past Pareto optimal solutions to approach the current Pareto optimal solutions.

According to (16), the associated linear equations for different periods can be approximated as

$$\psi_{n,c} \approx \phi_c \Lambda_{n,c} \text{ and } \psi_{n,p} \approx \phi_p \Lambda_{n,p} \tag{17}$$

where

$$\psi_{n,c} = \left[\bar{c}_{n,(i,j)}(t-1) \cdots \bar{c}_{n,(i,j)}(t-T+g+1)\right]^T$$

$$\phi_c = \begin{bmatrix} \bar{c}_{(i,j)}(t-2) & \cdots & \bar{c}_{(i,j)}(t-g-1) \\ \bar{c}_{(i,j)}(t-3) & \cdots & \bar{c}_{(i,j)}(t-g-2) \\ \vdots & \vdots & \vdots \\ \bar{c}_{(i,j)}(t-T+g) & \cdots & \bar{c}_{(i,j)}(t-T+1) \end{bmatrix}$$

$$\Lambda_{n,c} = \left[\lambda_{n,1,c} \cdots \lambda_{n,g,c}\right]^T$$

$$\psi_{n,p} = \left[\bar{P}_{n,(i,j)}(t-1) \cdots \bar{P}_{n,(i,j)}(t-T+g+1)\right]^T$$

$$\phi_p = \begin{bmatrix} \bar{P}_{(i,j)}(t-2) & \cdots & \bar{P}_{(i,j)}(t-g-1) \\ \bar{P}_{(i,j)}(t-3) & \cdots & \bar{P}_{(i,j)}(t-g-2) \\ \vdots & \vdots & \vdots \\ \bar{P}_{(i,j)}(t-T+g) & \cdots & \bar{P}_{(i,j)}(t-T+1) \end{bmatrix}$$

$$\Lambda_{n,p} = \left[\lambda_{n,1,p} \cdots \lambda_{n,g,p}\right]^T.$$

The least squares solutions to (17) can be expressed as

$$\Lambda_{n,c} \approx (\phi_c^T \phi_c)^{-1} \phi_c^T \psi_{n,c}$$
$$\Lambda_{n,p} \approx (\phi_p^T \phi_p)^{-1} \phi_p^T \psi_{n,p}. \tag{18}$$

Then, the variances of the approximation errors $\sigma^2_{n,(i,j),\bar{c}}$ and $\sigma^2_{n,(i,j),\bar{p}}$ in (16) are calculated as

$$\sigma^2_{n,(i,j),\bar{c}} = \frac{1}{T-g-1} \sum_{\zeta=t-T+g+1}^{t-1} \left[\bar{c}_{n,(i,j)}(\zeta) - \sum_{\tau=1}^{g} \lambda_{n,\tau,c} \bar{c}_{(i,j)}(\zeta-\tau) \right]^2$$
$$\sigma^2_{n,(i,j),\bar{p}} = \frac{1}{T-g-1} \sum_{\zeta=t-T+g+1}^{t-1} \left[\bar{P}_{n,(i,j)}(\zeta) - \sum_{\tau=1}^{g} \lambda_{n,\tau,p} \bar{P}_{(i,j)}(\zeta-\tau) \right]^2. \tag{19}$$

In summary, the centers $\bar{c}_{n,(i,j)}(t)$ and $\bar{P}_{n,(i,j)}(t)$ in (16) use $\lambda_{n,\tau,c}$ and $\lambda_{n,\tau,p}$ in (18), and use variances $\sigma^2_{n,(i,j),\bar{c}}$ of $\epsilon_{n,(i,j),\bar{c}}$ and $\sigma^2_{n,(i,j),\bar{p}}$ of $\epsilon_{n,(i,j),\bar{p}}$ in (19).

In Step 1.3, manifolds $\tilde{c}_{n,(i,j)}(t)$ and $\tilde{P}_{n,(i,j)}(t)$ are estimated as

$$\tilde{c}_{n,(i,j)}(t) = c_{n,(i,j)}(t-1) - \bar{c}_{(i,j)}(t-1) + \epsilon_{n,(i,j),\tilde{c}}$$
$$\tilde{P}_{n,(i,j)}(t) = P_{n,(i,j)}(t-1) - \bar{P}_{(i,j)}(t-1) + \epsilon_{n,(i,j),\tilde{p}} \tag{20}$$

where $\epsilon_{n,(i,j),\tilde{c}} \sim N(0, \sigma^2_{n,(i,j),\tilde{c}})$ and $\epsilon_{n,(i,j),\tilde{p}} \sim N(0, \sigma^2_{n,(i,j),\tilde{p}})$. The variances $\sigma^2_{n,(i,j),\tilde{c}}$ and $\sigma^2_{n,(i,j),\tilde{p}}$ are calculated as

$$\sigma^2_{n,(i,j),\tilde{c}} = (c_{n,(i,j)}(t-1) - \bar{c}_{(i,j)}(t-1))^2 + \min_{n'=1,\ldots,N_{\max}} (c_{n',(i,j)}(t-2) - \bar{c}_{(i,j)}(t-2))^2$$
$$\sigma^2_{n,(i,j),\tilde{p}} = (P_{n,(i,j)}(t-1) - \bar{P}_{(i,j)}(t-1))^2 + \min_{n'=1,\ldots,N_{\max}} (P_{n',(i,j)}(t-2) - \bar{P}_{(i,j)}(t-2))^2. \tag{21}$$

In Step 1.4, we repair the components of the points that are outside the boundary in accordance with the following:

$$c_{n,(i,j)}(t) := \begin{cases} \bar{c}_{n,(i,j)}(t) + \tilde{c}_{n,(i,j)}(t), & \text{if } c_{n,(i,j)}(t) \in (0,1] \\ c_{n,(i,j)}(t-1) + r_1(t)(1 - c_{n,(i,j)}(t-1)), & \text{otherwise} \end{cases} \tag{22}$$
$$P_{n,(i,j)}(t) := \begin{cases} \bar{P}_{n,(i,j)}(t) + \tilde{P}_{n,(i,j)}(t), & \text{if } P_{n,(i,j)}(t) \in [P^{\min}, P^{\max}] \\ P_{n,(i,j)}(t-1) + r_2(t)(1 - P_{n,(i,j)}(t-1)), & \text{otherwise} \end{cases}$$

where $r_1(t), r_2(t) \in [0,1]$ are random numbers. The discrete components $c_{n,(i,j)}(t)$ are then recovered using (23). Because the points are generated around the previous data points, the solution diversity of the prediction strategy can be reduced. To remedy this problem, we randomly generate some points in Step 2.

Algorithm 1: Hybrid Initialization ($t > 1$).

Input: Historical information of population $\Gamma(t-\rho)$ and available spectrum channel $\mathcal{M}(t-\rho)$, $\rho = 1, 2, \ldots, \min\{t-1, T\}$.
Parameters: Memory size T, reference quantity g, population size $N_{\max}$, and prediction parameter δ.
Output: $\Gamma(t)$.

if $t \leq T$ **then**
Database Construction: randomly generate half of $\Gamma(t)$ and the other half by randomly sampling the points from $\Gamma(t-1)$.
else
Step 1) Let $\Gamma'(t) = \emptyset$.
for $n = 1, 2, \ldots, N_{\max}$ **do**
Step 1.1) Perform boundary mapping.
For each $(i,j) \in \mathcal{L}$:

$$c_{n,(i,j)}(t-\rho) := \frac{c_{n,(i,j)}(t-\rho)}{|\mathcal{M}(t-\rho)|}$$

where $\rho = 1, 2, \ldots, \min\{t-1, T\}$.
Step 1.2) Perform center prediction.
For each $(i,j) \in \mathcal{L}$:
Generate components $\bar{c}_{n,(i,j)}(t)$ and $\bar{P}_{n,(i,j)}(t)$ of $\boldsymbol{x}_n(t)$ using (16) with coefficient vectors $\Lambda_{n,c}$ and $\Lambda_{n,p}$ in (18) and variances $\sigma^2_{n,(i,j),\bar{c}}$ and $\sigma^2_{n,(i,j),\bar{p}}$ in (19) for all $(i,j) \in \mathcal{L}$.
Step 1.3) Manifold Estimation: generate components $\tilde{c}_{n,(i,j)}(t)$ and $\tilde{P}_{n,(i,j)}(t)$ of $\boldsymbol{x}_n(t)$ using (20) with variances $\sigma^2_{n,(i,j),\tilde{c}}$ and $\sigma^2_{n,(i,j),\tilde{p}}$ in (21).
Step 1.4) Perform boundary demapping.
For each $(i,j) \in \mathcal{L}$:
Generate components $c_{n,(i,j)}(t)$ and $P_{n,(i,j)}(t)$ of $\boldsymbol{x}_n(t)$ using (22); assign

$$c_{n,(i,j)}(t) := \lceil c_{n,(i,j)}(t) |\mathcal{M}(t)| \rceil \tag{23}$$

where $\lceil \cdot \rceil$ denotes the ceiling function. Add $\boldsymbol{x}_n(t)$ to $\Gamma'(t)$.
end for
Step 2) Point Generation: randomly sample $\delta N_{\max}$ points from $\Gamma'(t)$, and randomly generate additional $(1-\delta)N_{\max}$ points to produce $\Gamma(t)$.
end if

Algorithms 2 and 3 present our crossover and mutation designs that are applied to the points representing the values of the decision variable vector $\boldsymbol{x}_n(t,k)$ with iteration k. For discrete decision variables $c_{n,(i,j)}(t,k)$, the crossover operation is performed in an element-by-element manner. Two components of distinct points that are randomly selected from the population are swapped based on a random binary integer. Although the mutation operation is a vector-based method, a few discrete components of the points are randomly selected and shuffled. For the continuous decision variable $P_{n,(i,j)}(t,k)$, both crossover and mutation operation apply a modified Laplace genetic operation [44]. The truncated Laplacian random variable $\beta(t,k)$ in

Algorithm 2: Crossover Operation.

Input: $\boldsymbol{x}_{n'}(t,k)$ and $\boldsymbol{x}_{n''}(t,k)$.
Output: $\boldsymbol{x}_n(t,k)$.
For each $(i,j) \in \mathcal{L}$:
Assign

$$c_{n,(i,j)}(t,k) := \begin{cases} c_{n,'(i,j)}(t,k), & \text{if } d=0 \\ c_{n,''(i,j)}(t,k), & \text{if } d=1 \end{cases} \tag{24}$$

where d is a random binary number and $c_{n,'(i,j)}(t,k)$ and $c_{n,''(i,j)}(t,k)$ are discrete components of $\boldsymbol{x}_{n'}(t,k)$ and $\boldsymbol{x}_{n''}(t,k)$, respectively.
Assign

$$\begin{aligned} P_{n,(i,j)}(t,k) := \frac{1}{1+\beta(t,k)}(P_{n'(i,j)}(t,k) \\ + \beta(t,k)|P_{n,'(i,j)}(t,k) - P_{n,''(i,j)}(t,k)| \\ - P^{\min}) + P^{\min} \end{aligned} \tag{25}$$

where $\beta(t,k) \in [0,1]$ is a truncated Laplacian random variable, and $P_{n,'(i,j)}(t,k)$ and $P_{n,''(i,j)}(t,k)$ are continuous components of $\boldsymbol{x}_{n'}(t,k)$ and $\boldsymbol{x}_{n''}(t,k)$, respectively.

Algorithm 3: Mutation Operation.

Input: $\boldsymbol{x}_{n'}(t,k)$.
Output: $\boldsymbol{x}_n(t,k)$.
Discrete components $c_{n,(i,j)}(t,k)$ of $\boldsymbol{x}_n(t,k)$ are the same as those of $\boldsymbol{x}_{n'}(t,k)$ except that $\lceil |\mathcal{L}|/2 \rceil$ components are randomly selected and shuffled.
Continuous components $P_{n,(i,j)}(t,k)$ of $\boldsymbol{x}_n(t,k)$ are generated by (25), where $P_{n,'(i,j)}(t,k)$ is obtained from $\boldsymbol{x}_{n'}(t,k)$ and $P_{n,''(i,j)}(t,k)$ is randomly generated from $[P^{\min}, P^{\max}]$.

Step 1 is generated by Laplace$(0,1)$ with a truncated interval $[-5,5]$, and transformed into the interval $[0,1]$.

In Algorithms 2 and 3, points are generated and satisfy (3). However, they can violate the constraint in (6) due to the inappropriate spectrum allocation. To address this problem, Algorithm 4 presents a heuristic adjustment method for repairing the infeasible points. In Step 2, if the link in $\boldsymbol{x}_{n'}(t,k)$ violates the constraint in (6), then the reallocation operation is applied. Thus, the violation condition can be alleviated without degrading the objective value of (13). If the link still violates the constraint, we replace $\boldsymbol{x}_{n'}(t,k)$ with a feasible point that is randomly selected from the population in Step 3. In Step 4, we perform a hypermutation operation. Because the SINR values remain constant, the feasibility of the solution can be maintained during the evolution process, as shown in Theorem 1.

Theorem 1: Algorithms 2 and 4 produce $\boldsymbol{x}_n(t,k)$ that satisfies (3) and (6).

Proof: For any given network topology, the condition in (3) is satisfied according to (25). The SINR function in (5) can be

Algorithm 4: Adjustment Operation.

Input: Infeasible $\boldsymbol{x}_{n'}(t,k)$ and feasible $\boldsymbol{x}_{n''}(t,k)$.
Output: $\boldsymbol{x}_n(t,k)$.
Step 1)
For each $(i,j) \in \mathcal{L}$:
Evaluate $\text{SINR}_{(i,j)}(t,k)$ associated with $\boldsymbol{x}_{n'}(t,k)$ using (5).
Step 2)
For each $(i,j) \in \mathcal{L}$:
Substitute the discrete component $c_{n,'(i,j)}(t,k)$ of $\boldsymbol{x}_{n'}(t,k)$ with another component $c_{n,'(i,'j')}(t,k)$ if $\text{SINR}_{(i,j)}(t,k) < \gamma$, where

$$1 \le |\mathcal{L}_{c_{n,'(i,'j')}(t,k)}| \le |\mathcal{L}_{c_{n,'(i,j)}(t,k)}| - m$$

for some positive interger m.
Step 3) Assign $\boldsymbol{x}_n(t,k) := \boldsymbol{x}_{n'}(t,k)$.
For each $(i,j) \in \mathcal{L}$:
Evaluate $\text{SINR}_{(i,j)}(t,k)$ associated with $\boldsymbol{x}_n(t,k)$ using (5); assign $\boldsymbol{x}_n(t,k) := \boldsymbol{x}_{n''}(t,k)$ if $\text{SINR}_{(i,j)}(t,k) < \gamma$.
Step 4) Select two different sets of links with the same size and swap their components; if $|\mathcal{L}_{c_{n,(i,j)}(t,k)}| = |\mathcal{L}_{c_{n,(i,'j')}(t,k)}|$, then allocate the spectrum channel $c_{n,(i,'j')}(t,k)$ to link (i,j) associated with $\boldsymbol{x}_n(t,k)$.

simplified as

$$\text{SINR}_{(i,j)}(t,k) = \frac{P_{n,'(i,j)}(t,k)}{\frac{\epsilon_0}{\omega_1} + \omega_2 \sum_{(a,b)\in\mathcal{L}_{c_{n,'(i,j)}(t,k)}\setminus\{(i,j)\}} P_{n,'(a,b)}(t,k)}$$

for all $(i,j) \in \mathcal{L}$, where ω_1 and ω_2 are the path loss constants. The reallocation operation in Step 2 of Algorithm 4 decreases the size of $\mathcal{L}_{c_{n,'(i,j)}(t,k)}$, increasing $\text{SINR}_{(i,j)}(t,k)$. In the hypermutation operation in Step 4, $\text{SINR}_{(i,j)}(t,k)$ remains constant because $|\mathcal{L}_{c_{n,(i,j)}(t,k)}| = |\mathcal{L}_{c_{n,(i,'j')}(t,k)}|$. We thus have

$$\begin{aligned} \text{SINR}_{(i,j)}(t,k) &= \frac{P_{n,(i,j)}(t,k)}{\frac{\epsilon_0}{\omega_1} + \omega_2 \sum_{(a,b)\in\mathcal{L}_{c_{n,(i,j)}(t,k)}\setminus\{(i,j)\}} P_{n,(a,b)}(t,k)} \\ &= \frac{P_{n,(i,j)}(t,k)}{\frac{\epsilon_0}{\omega_1} + \omega_2 \sum_{(a,b)\in\mathcal{L}_{c_{n,(i,'j')}(t,k)}\setminus\{(i,'j')\}} P_{n,(a,b)}(t,k)} \ge \gamma \end{aligned}$$

which maintains the feasibility of the solution. ■

Using Algorithms 1–4, Algorithm 5 presents our dynamic multiobjective approach to resource allocation in the CR network. Algorithm 5 approximates the Pareto set and associated Pareto front with a finite number of points. The initial points are generated by Algorithm 1. A tournament selection [45] is then applied to create a mating pool in which the genetic operations presented in Algorithms 2 and 3 are performed. Algorithm 4 ensures that all points are feasible; otherwise, the adjustment

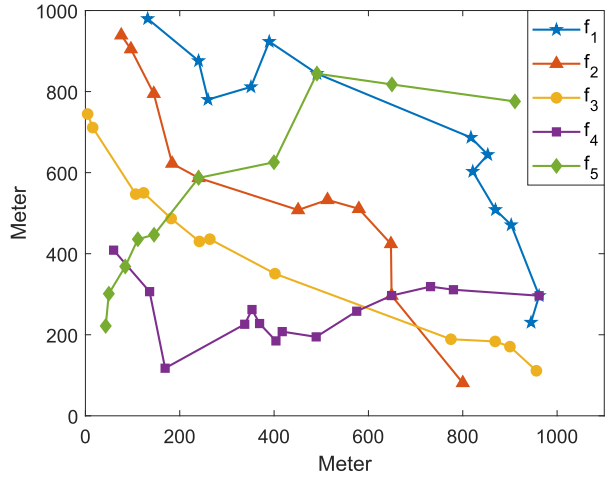

Fig. 2. Network topology of a CR network.

operation is conducted. If too many points are obtained, any update methods for an archive can be used to remove a few nondominated points. Finally, the approximate Pareto front and set are obtained, and a final solution, termed a knee solution, which achieves excellent overall performance in meeting the objectives, can be selected using the minimum Manhattan distance approach [46].

Remark 4: Conventional algorithms and the proposed algorithm use the Pareto rank in the evolution process, yielding a time complexity that is approximately equal to that of [47]

$$O(2k_{\max}N_{\max}(t_{\text{com}}+N_{\max}-1)) \tag{26}$$

where t_{com} represents the average computational time for an objective evaluation. With the same complexity, the proposed algorithm can efficiently generate feasible solutions in the evolution process, as shown in Theorem 1.

Remark 5: This article assumes that the nodes are static, which has been the general setting in most relevant studies; however, the proposed approach can be applied to a scenario in which dynamic nodes are involved if their positions change gradually. In this scenario, the concept of dynamically tracking new Pareto optimal solutions using historical data remains valid. This is because the previous positions of dynamic nodes may differ little from their current positions, and therefore, new Pareto solutions for resource allocation can be close to the past Pareto solutions. The proposed approach becomes invalid if the nodes are rapidly changing their positions, as in the case of vehicular communication networks. In this case, complete multiobjective optimization must be performed in each period, which substantially impairs the algorithm's efficiency.

IV. Numerical Results

This section presents a numerical analysis that we conducted for the proposed multiobjective approach for resource allocation in a CR network. Fig. 2 shows the network topology adopted in our simulations, which is similar to the scenario considered in [19] and [48]. In the figure, $|\mathcal{N}|=60$ nodes are randomly

Algorithm 5: Dynamic Resource Allocation.

Input: Dynamic MOP in (14); $\Gamma(t-\rho)$, $\mathcal{M}(t-\rho)$, and $\boldsymbol{x}^*(t-\rho)$ for $\rho=1,2,\ldots,\min\{t-1,T\}$ if $t>1$.
Parameters: Memory size T, reference quantity g, population size $N_{\max}$, prediction parameter δ, and maximum iteration $k_{\max}$.
Output: Approximate Pareto set $\Gamma(t)$ and knee $\boldsymbol{x}^*(t)$.
if $t>1$ and $\mathcal{M}(t)=\mathcal{M}(t-1)$ **then**
Memory Maintenance: Let $\Gamma(t)=\Gamma(t-1)$ and $\boldsymbol{x}^*(t)=\boldsymbol{x}^*(t-1)$.
else
Step 1) Population Initialization: Use Algorithm 1 to generate $\Gamma(t)$ if $t>1$; otherwise, randomly generate points to produce $\Gamma(t)$.
Step 2) Evolution: let $\Gamma(t,k)=\Gamma(t)$.
for $k=1,2,\ldots,k_{\max}$ **do**
Step 2.1) Use tournament selection over $\Gamma(t,k)$ to create a mating pool. Apply crossover and mutation operations in Algorithms 2 and 3 to the mating pool with rate μ and $1-\mu$, respectively. Add the offspring and mutants to $\Gamma(t,k)$. For an infeasible $\boldsymbol{x}_{n'}(t,k)\in\Gamma(t,k)$, randomly select a feasible point $\boldsymbol{x}_{n''}(t,k)\in\Gamma(t,k)$ and apply Algorithm 4 to produce a feasible point $\boldsymbol{x}_n(t,k)\in\Gamma(t,k)$.
Step 2.2) Remove the dominated points from $\Gamma(t,k)$. Use an update method for archives to reduce the size if $|\Gamma(t,k)|>N_{\max}$.
end for
Step 3) Knee selection: Select the knee $\boldsymbol{x}^*(t)$ on the basis of the approximate Pareto front and the associated Pareto set $\Gamma(t,k_{\max})$. Let $\Gamma(t)=\Gamma(t,k_{\max})$.
end if

deployed over a 1000 m $\times$ 1000 m area; there are $|\mathcal{L}|=55$ links between nodes and $|\mathcal{F}|=5$ data flows in the network. The number of available spectrum channels is $|\mathcal{M}(t)|\in(10,25)$. The transition rates $\mu=1.1$ and $\lambda=1.2$ in (1) were set as those in [5] and [14]. Most of the following parameters were chosen in accordance with [13] and [19]: power consumption bounds $P^{\min}=10$ mW and $P^{\max}=30$ mW; antenna gains $G_i^{\text{Tx}}=G_j^{\text{Rx}}=1$, $\forall i,j\in\mathcal{N}$; path loss exponent $\alpha=3$; additive white Gaussian noise (AWGN) variance $\sigma_0^2=1$; SINR threshold $\gamma=10$ dB; and channel bandwidth $B=5$ MHz.

For the performance evaluation, the proposed approach was compared with conventional multiobjective evolutionary algorithms and single-objective optimization methods, which were, specifically, the SPEA-II and NSGA-II with fixed power methods modified from the work in [19]; NSGA-II method modified from the work in [21]; modified fairness minimization (FairMin) method based on the work in [49] and [50]; modified energy efficiency maximization method (EEMax) based on the work in [12], [51], and [52]; and spectrum utilization maximization (SpecMax) method modified from the work in [13]. Given the tradeoff between solution diversity and algorithm efficiency in

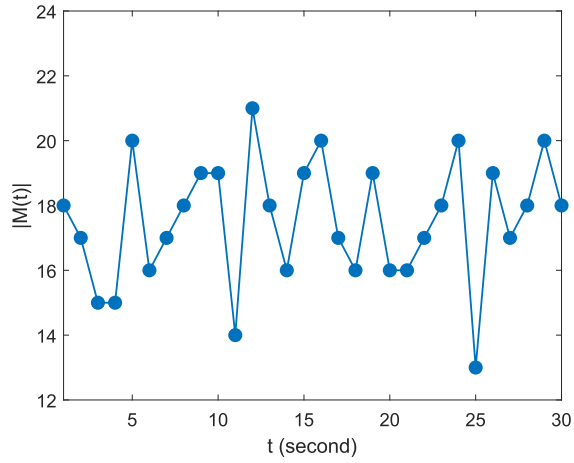

(a)

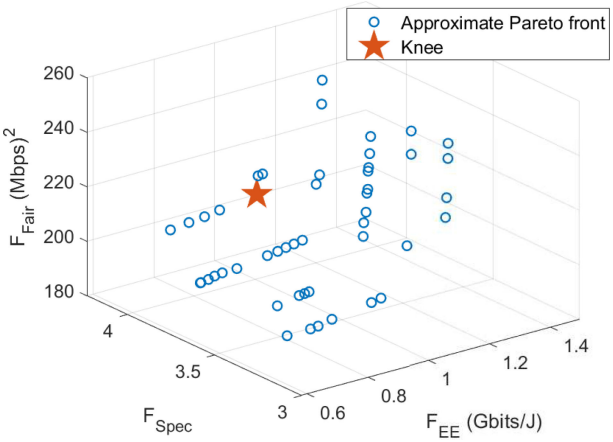

(b)

Fig. 3. (a) Dynamic spectrum resources. (b) Sample Pareto front and knee at $t = 1$.

TABLE II
COMPARISON OF EXISTING RESOURCE ALLOCATION METHODS

Compared with respect to proposed algorithm ($\delta = 0.5$)			
Methods	Energy efficiency	Fairness	Spectrum utilization
Proposed, $\delta = 0$	0.49%	0.07%	-1.26%
Proposed, $\delta = 1$	-0.13%	5.84%	-4.37%
NSGA-II	-41.47%	13.85%	-32.88%
NSGA-II with fixed power	-46.45%	33.24%	-24.74%
SPEA-II with fixed power	-46.89%	35.33%	-20.19%
EEMax	3.86%	38.73%	-31.4%
FairMin	-50.33%	-13.17%	-26.89%
SpecMax	-50.2%	32.33%	13.16%
Average	-28.89%	18.28%	-16.07%

Algorithm 1, we assigned different values to the prediction parameter δ: when $\delta = 0$, only random generation was applied; when $\delta = 1$, only the prediction strategy was applied; when $\delta = 0.5$, both random generation and the prediction strategy were applied.

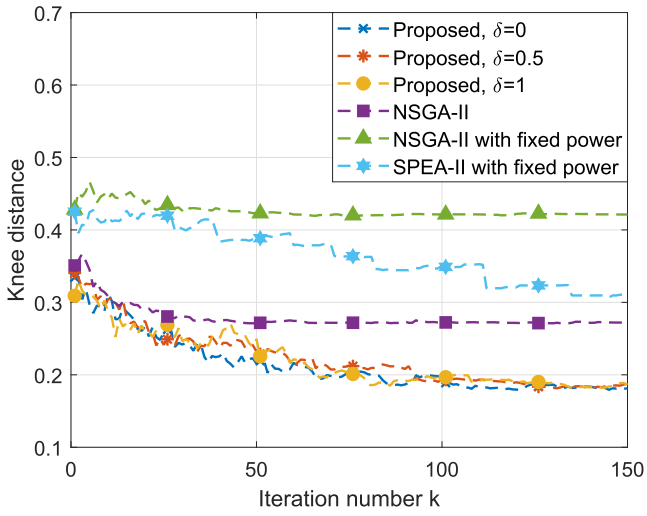

(a)

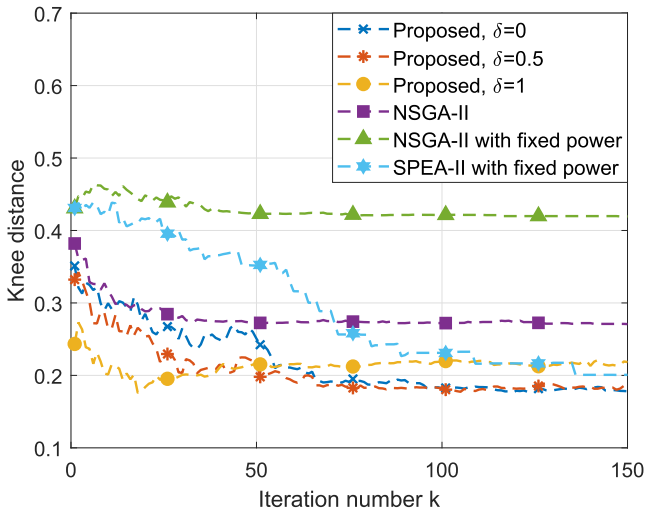

(b)

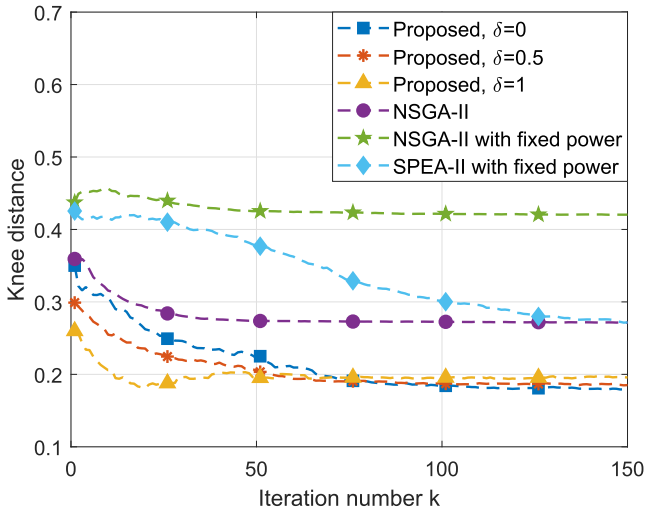

(c)

Fig. 4. Convergence analysis of multiobjective evolutionary algorithms for the dynamic spectrum resource scheme shown in Fig. 3(a). (a) $t = 1$. (b) $t = 25$. (c) Average performance over iterations.

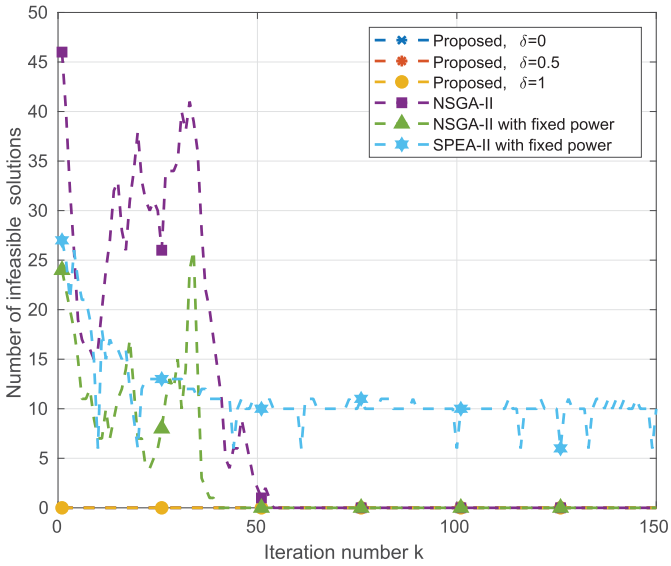

Fig. 5. Number of infeasible solutions during the evolution process.

Remark 6: Both SPEA-II and NSGA-II with fixed power were multiobjective evolutionary algorithms used to solve

$$\max_{c_{(i,j)}(t)} \quad \forall(i,j)\in\mathcal{L} \; F_{\text{EE}}(c_{(i,j)}(t)) - \eta D(c_{(i,j)}(t))$$

$$\max_{c_{(i,j)}(t)} \quad \forall(i,j)\in\mathcal{L} \; F_{\text{Spec}}(c_{(i,j)}(t)) - \eta D(c_{(i,j)}(t))$$

$$\text{subject to } (6) \tag{27}$$

where

$$D(c_{(i,j)}(t)) = \max\{\gamma - \text{SINR}_{(i,j)}(t), 0\}.$$

If $D(c_{(i,j)}(t)) > 0$, then $c_{(i,j)}(t)$ is infeasible. In (27), only the decision variables representing the spectrum allocation of links were to be determined (i.e., the power usage was fixed). In addition, Algorithms 2 and 3 were used for genetic operations.

For a convergence analysis of the multiobjective methods, a normalized knee distance value that ought to decrease over the iterations was used for evaluating the convergence [46]. The autoregression model in Algorithm 1 was designed using a memory size $T = 10$ and reference quantity $g = 3$. Our dynamic multiobjective approach was realized using Algorithm 5 with a population size $N_{\max} = 50$, prediction parameter $\delta = 0.5$, maximum iteration $k_{\max} = 150$, crossover probability $\mu = 0.9$, and mutation probability $1 - \mu = 0.1$. Fig. 3(a) and (b) presents a realization of the dynamic spectrum resources and a sample Pareto front, respectively. The algorithm convergence was examined at periods $t = 1$ and $t > 1$. When $t = 1$, no historical information existed and only feasible search mechanisms were used by our approach. This setting examined direct optimization without considering the dynamic characteristic of the CR-based network. When $t > 1$, the number of available channels changed over two consecutive periods. In this setting, historical data can be used to improve the convergence rate, leading to a dynamic MOP.

Fig. 4(a) shows the algorithm convergence rates and levels at $t = 1$. Our approach yielded the best convergence levels among all multiobjective methods, as indicated by the smaller knee distances attained. This is attributable to our feasible search mechanisms, which can efficiently determine the feasible points unlike conventional penalty methods that are developed for constraint handling. The different values of δ in the proposed approach had no real effect on our algorithm's performance, which was due to a lack of historical data, leading to similar convergence rates and levels. For the other setting, Fig. 4(b) shows the numerical results sampled at $t = 25$. The proposed approach outperformed the comparable methods in terms of the rate and level of convergence; the comparable methods initialized the population randomly without accounting for the

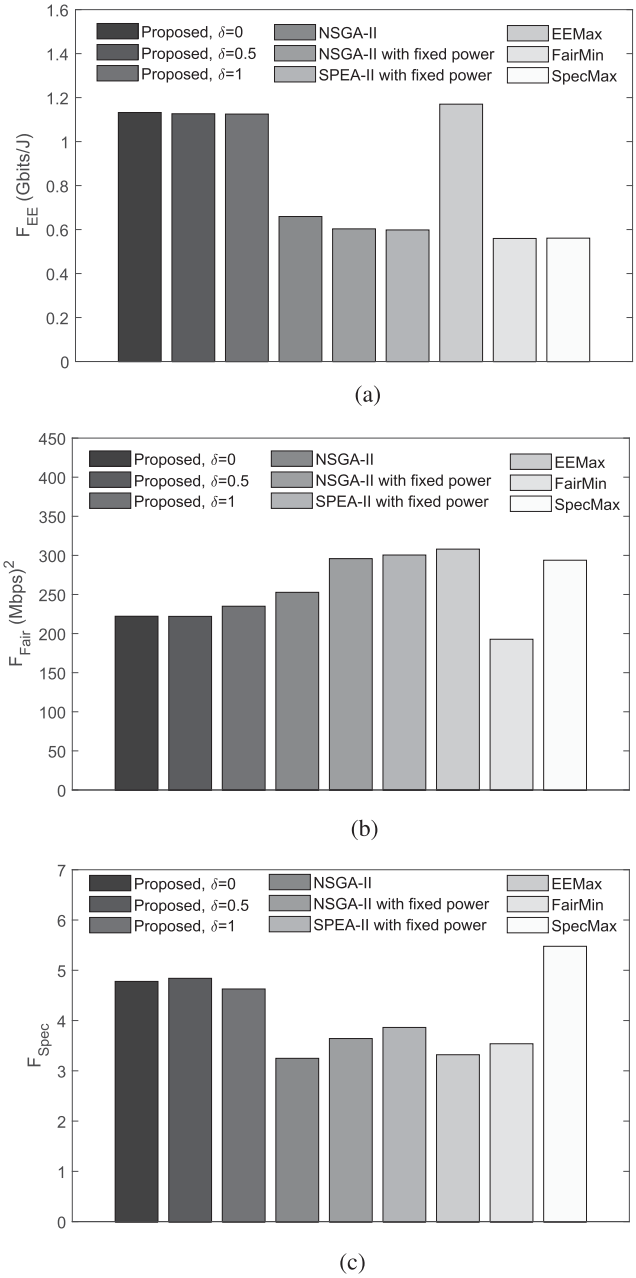

Fig. 6. Average objective values of various methods over the observed time period. (a) Energy efficiency. (b) Fairness. (c) Spectrum utilization.

information available from the previous optimization. The convergence rate of our proposed method was affected by δ: a larger δ yielded faster convergence because more historical data were used for the prediction. Conversely, the convergence level was slightly degraded for a large δ value because it incurred less solution diversity. The parameter δ can, thus, be tuned to balance the convergence rate and level as desired. Fig. 4(c) presents the average convergence performance over a given period with consistent observations.

Under the same time complexity as that observed in (26), Fig. 5 shows the number of infeasible solutions obtained for the comparable algorithms in each iteration. With the same population size, the number of infeasible solutions at different iteration numbers represents the efficiency of the algorithms in the exploration. The proposed approach was efficient, as indicated by its production of feasible points under all conditions; our method could do so because of our proposed mechanism for feasible generation. The comparable methods were less efficient in the exploration. The following two findings can be observed from Fig. 5. First, both NSGA-II and SPEA-II with fixed power had fewer decision variables to be determined than NSGA-II. Fewer decision variables implied fewer constraints to be satisfied, leading to fewer infeasible points when they were randomly generated. As such, when the initial populations were generated ($k = 1$), the two methods using a fixed power yielded fewer infeasible points than NSGA-II did. Second, the number of infeasible points produced by NSGA-II with or without fixed power eventually approached zero, whereas this number was not reduced in SPEA-II with fixed power.

Fig. 6 shows the average performance in terms of the objectives, whose numerical values are summarized in Table II. The single-objective optimization methods achieved the best performance in their individual dimensions but performed the worst in other dimensions. The proposed approach outperformed the comparable multiobjective methods, with all these methods striking a balance between the objectives; moreover, our method attained performance that was close to that achieved by single-objective optimization methods on each objective.

V. Conclusion

This article focused on power and spectrum allocation and considered the energy efficiency, fairness, and spectrum utilization of CR networks. The following conclusions were drawn.

1) A dynamic MOP was formulated, in which the available spectrum channels varied over time and multiple objectives were involved. To solve the MOP, we proposed a dynamic multiobjective resource allocation algorithm comprising a hybrid initialization method and feasible point generation mechanisms.
2) A theoretical analysis for Theorem 1 was conducted to verify the feasibility-preserving mechanisms in Algorithm 4. The theorem is based on the concept that a crossover operation is applied to meet the power constraints and that an adjustment method for the set of links is applied to meet the SINR constraint. By conducting these operations sequentially, our algorithm guaranteed a feasible generation of random points.
3) Our proposed approach maintained a satisfactory balance between all objectives and yielded a better convergence rate and level than existing multiobjective methods.
4) The proposed approach was considered valid if the CR networks were composed of static or dynamic sensing nodes that only changed their positions gradually. Further research is required to formulate a multiobjective approach for resource allocation in a rapidly time-varying network topology, e.g., a vehicular communication network.

References

[1] A. Aijaz and A. H. Aghvami, "Cognitive machine-to-machine communications for Internet-of-Things: A protocol stack perspective," *IEEE Internet Things J.*, vol. 2, no. 2, pp. 103–112, Apr. 2015.

[2] C. Perera, A. Zaslavsky, P. Christen, and D. Georgakopoulos, "Context aware computing for the Internet of Things: A survey," *IEEE Commun. Surv. Tut.*, vol. 16, no. 1, pp. 414–454, Jan.–Mar. 2014.

[3] P. Rawat, K. D. Singh, and J. M. Bonnin, "Cognitive radio for M2M and Internet of Things: A survey," *Comput. Commun.*, vol. 94, pp. 1–29, Nov. 2016.

[4] S. Byun, I. Balasingham, and X. Liang, "Dynamic spectrum allocation in wireless cognitive sensor networks: Improving fairness and energy efficiency," in *Proc. IEEE Veh. Technol. Conf.*, Sep. 2008, pp. 1–5.

[5] J. Ren, Y. Zhang, N. Zhang, D. Zhang, and X. Shen, "Dynamic channel access to improve energy efficiency in cognitive radio sensor networks," *IEEE Trans. Wireless Commun.*, vol. 15, no. 5, pp. 3143–3156, May 2016.

[6] S. Haykin, "Cognitive radio: Brain-empowered wireless communications," *IEEE J. Sel. Areas Commun.*, vol. 23, no. 2, pp. 201–220, Feb. 2005.

[7] A. Ahmad, S. Ahmad, M. H. Rehmani, and N. U. Hassan, "A survey on radio resource allocation in cognitive radio sensor networks," *IEEE Commun. Surv. Tut.*, vol. 17, no. 2, pp. 888–917, Apr.–Jun. 2015.

[8] J. M. Alfonso and L. B. Agudelo, "Centralized spectrum broker and spectrum sensing with compressive sensing techniques for resource allocation in cognitive radio networks," in *Proc. IEEE Latin-America Conf. Commun.*, Nov. 2013, pp. 1–6.

[9] C. Park, S. Kim, S. Lim, and M. Song, "HMM based channel status predictor for cognitive radio," in *Proc. Asia-Pacific Microw. Conf.*, Dec. 2007, pp. 1–4.

[10] K. W. Choi and E. Hossain, "Estimation of primary user parameters in cognitive radio systems via hidden Markov model," *IEEE Trans. Signal Process.*, vol. 61, no. 3, pp. 782–795, Feb. 2013.

[11] V. K. Tumuluru, P. Wang, and D. Niyato, "A neural network based spectrum prediction scheme for cognitive radio," in *Proc. IEEE Int. Conf. Commun.*, May 2010, pp. 1–5.

[12] M. Cui, B. Hu, X. Li, H. Chen, S. Hu, and Y. Wang, "Energy-efficient power control algorithms in massive MIMO cognitive radio networks," *IEEE Access*, vol. 5, pp. 1164–1177, 2017.

[13] P. Bhardwaj *et al.*, "Enhanced dynamic spectrum access in multiband cognitive radio networks via optimized resource allocation," *IEEE Trans. Wireless Commun.*, vol. 15, no. 12, pp. 8093–8106, Dec. 2016.

[14] D. Zhang *et al.*, "Energy-harvesting-aided spectrum sensing and data transmission in heterogeneous cognitive radio sensor network," *IEEE Trans. Veh. Technol.*, vol. 66, no. 1, pp. 831–843, Jan. 2017.

[15] C. C. Zarakovitis and Q. Ni, "Maximizing energy efficiency in multiuser multicarrier broadband wireless systems: Convex relaxation and global optimization techniques," *IEEE Trans. Veh. Technol.*, vol. 65, no. 7, pp. 5275–5286, Jul. 2016.

[16] B. Gu, C. Zhang, H. Wang, Y. Yao, and X. Tan, "Power control for cognitive M2M communications underlaying cellular with fairness concerns," *IEEE Access*, vol. 7, pp. 80789–80799, 2019.

[17] N. Zhao, F. R. Yu, H. Sun, and M. Li, "Adaptive power allocation schemes for spectrum sharing in interference-alignment-based cognitive radio networks," *IEEE Trans. Veh. Technol.*, vol. 65, no. 5, pp. 3700–3714, May 2016.

[18] M. R. Mili, L. Musavian, K. A. Hamdi, and F. Marvasti, "How to increase energy efficiency in cognitive radio networks," *IEEE Trans. Commun.*, vol. 64, no. 5, pp. 1829–1843, May 2016.

[19] R. Han, Y. Gao, C. Wu, and D. Lu, "An effective multi-objective optimization algorithm for spectrum allocations in the cognitive-radio-based Internet of Things," *IEEE Access*, vol. 6, pp. 12858–12867, 2018.
[20] N. Zhang, H. Liang, N. Cheng, Y. Tang, J. W. Mark, and X. S. Shen, "Dynamic spectrum access in multi-channel cognitive radio networks," *IEEE J. Sel. Areas Commun.*, vol. 32, no. 11, pp. 2053–2064, Nov. 2014.
[21] Z. Wei and B. Hu, "A fair multi-channel assignment algorithm with practical implementation in distributed cognitive radio networks," *IEEE Access*, vol. 6, pp. 14 255–14267, 2018.
[22] A. Alabbasi, Z. Rezki, and B. Shihada, "Energy efficient resource allocation for cognitive radios: A generalized sensing analysis," *IEEE Trans. Wireless Commun.*, vol. 14, no. 5, pp. 2455–2469, May 2015.
[23] J. A. Ansere, G. Han, H. Wang, C. Choi, and C. Wu, "A reliable energy efficient dynamic spectrum sensing for cognitive radio IoT networks," *IEEE Access*, vol. 6, pp. 6748–6759, 2019.
[24] M. Nitti, M. Murroni, M. Fadda, and L. Atzori, "Exploiting social Internet of things features in cognitive radio," *IEEE Access*, vol. 4, pp. 9204–9212, 2016.
[25] H. Shi, R. V. Prasad, E. Onur, and I. G. M. M. Niemegeers, "Fairness in wireless networks: Issues, measures and challenges," *IEEE Commun. Surv. Tut.*, vol. 16, no. 1, pp. 5–24, Jan.–Mar. 2014.
[26] S. He, Y. Huang, L. Yang, B. Ottersten, and W. Hong, "Energy efficient coordinated beamforming for multicell system: Duality-based algorithm design and massive MIMO transition," *IEEE Trans. Commun.*, vol. 63, no. 12, pp. 4920–4935, Dec. 2015.
[27] J. An, Y. Zhang, X. Gao, and K. Yang, "Energy-efficient base station association and beamforming for multi-cell multiuser systems," *IEEE Trans. Wireless Commun.*, vol. 19, no. 4, pp. 2841–2854, Apr. 2020.
[28] Y. Hao, Q. Ni, H. Li, and S. Hou, "On the energy and spectral efficiency tradeoff in massive MIMO-enabled HetNets with capacity-constrained backhaul links," *IEEE Trans. Commun.*, vol. 65, no. 11, pp. 4720–4733, Nov. 2017.
[29] Y. Hao, Q. Ni, H. Li, and S. Hou, "Robust multi-objective optimization for EE-SE tradeoff in D2D communications underlaying heterogeneous networks," *IEEE Trans. Commun.*, vol. 66, no. 10, pp. 4936–4949, Oct. 2018.
[30] M. Naeem, A. Anpalagan, M. Jaseemuddin, and D. C. Lee, "Resource allocation techniques in cooperative cognitive radio networks," *IEEE Commun. Surv. Tut.*, vol. 16, no. 2, pp. 729–744, Apr.–Jun. 2014.
[31] H.-H. Chang, W.-Y. Chiu, H. Sun, and C.-M. Chen, "User-centric multi-objective approach to privacy preservation and energy cost minimization in smart home," *IEEE Syst. J.*, vol. 13, no. 1, pp. 1030–1041, Mar. 2019.
[32] K. K. Anumandla, B. Akella, S. L. Sabat, and S. K. Udgata, "Spectrum allocation in cognitive radio networks using multi-objective differential evolution algorithm," in *Proc. Int. Conf. Signal Process. Integr. Netw.*, Feb. 2015, pp. 264–269.
[33] O. Yeniay, "Penalty function methods for constrained optimization with genetic algorithms," *Math. Comput. Appl.*, vol. 10, no. 1, pp. 45–56, 2005.
[34] R. Azzouz, S. Bechikh, and L. B. Said, "Dynamic multi-objective optimization using evolutionary algorithms: A survey," *Recent Adv. Evol. Multi-objective Optim.*, vol. 20Aug. 2017, pp. 31–70.
[35] A. Zhou, Y. Jin, and Q. Zhang, "A population prediction strategy for evolutionary dynamic multiobjective optimization," *IEEE Trans. Cybern.*, vol. 44, no. 1, pp. 40–53, Jan. 2014.
[36] B. Xu, Y. Zhang, D. Gong, Y. Guo, and M. Rong, "Environment sensitivity-based cooperative co-evolutionary algorithms for dynamic multi-objective optimization," *IEEE/ACM Trans. Comput. Biol. Bioinf.*, vol. 15, no. 6, pp. 1877–1890, Nov. 2018.
[37] J. Zhu, Y. Song, D. Jiang, and H. Song, "Multi-armed bandit channel access scheme with cognitive radio technology in wireless sensor networks for the Internet of Things," *IEEE Access*, vol. 4, pp. 4609–4617, 2016.
[38] W. Ejaz and M. Ibnkahla, "Multiband spectrum sensing and resource allocation for IoT in cognitive 5G networks," *IEEE Internet Things J.*, vol. 5, no. 1, pp. 150–163, Feb. 2018.
[39] P. Lin, J. Jia, Q. Zhang, and M. Hamdi, "Dynamic spectrum sharing with multiple primary and secondary users," *IEEE Trans. Veh. Technol.*, vol. 60, no. 4, pp. 1756–1765, May 2011.
[40] Y. Mao and D. Cheng, "A localization algorithm by dynamic path-loss fading index for intelligent mining system," in *Proc. Int. Conf. Comput. Sci. Educ.*, Aug. 2014, pp. 977–980.
[41] M. Costa and A. Ephremides, "Energy efficiency versus performance in cognitive wireless networks," *IEEE J. Sel. Areas Commun.*, vol. 34, no. 5, pp. 1336–1347, May 2016.
[42] J. Cho, Y. Wang, I. Chen, K. S. Chan, and A. Swami, "A survey on modeling and optimizing multi-objective systems," *IEEE Commun. Surv. Tut.*, vol. 19, no. 3, pp. 1867–1901, Jul.–Sep. 2017.
[43] Z. Fei, B. Li, S. Yang, C. Xing, H. Chen, and L. Hanzo, "A survey of multi-objective optimization in wireless sensor networks: Metrics, algorithms, and open problems," *IEEE Commun. Surv. Tut.*, vol. 19, no. 1, pp. 550–586, Jan.–Mar. 2017.
[44] K. Deep and M. Thakur, "A new crossover operator for real coded genetic algorithm," *Appl. Math. Comput.*, vol. 188, no. 1, pp. 895–911, 2007.
[45] K. Deb, A. Pratap, S. Agarwal, and T. Meyarivan, "A fast and elitist multiobjective genetic algorithm: NSGA-II," *IEEE Trans. Evol. Comput.*, vol. 6, no. 2, pp. 182–197, Apr. 2002.
[46] W.-Y. Chiu, G. G. Yen, and T.-K. Juan, "Minimum manhattan distance approach to multiple criteria decision making in multiobjective optimization problems," *IEEE Trans. Evol. Comput.*, vol. 20, no. 6, pp. 972–985, Dec. 2016.
[47] C. A. C. Coello, G. B. Lamont, and D. A. Van Veldhuizen, *Evolutionary Algorithms for Solving Multi-Objective Problems*. Berlin, Germany: Springer, 2007.
[48] M. R. Mili and L. Musavian, "Interference efficiency: A new metric to analyze the performance of cognitive radio networks," *IEEE Trans. Wireless Commun.*, vol. 16, no. 4, pp. 2123–2138, Apr. 2017.
[49] S. S. Kalamkar, J. P. Jeyaraj, A. Banerjee, and K. Rajawat, "Resource allocation and fairness in wireless powered cooperative cognitive radio networks," *IEEE Trans. Commun.*, vol. 64, no. 8, pp. 3246–3261, Aug. 2016.
[50] F. Zhou, N. C. Beaulieu, J. Cheng, Z. Chu, and Y. Wang, "Robust max-min fairness resource allocation in sensing-based wideband cognitive radio with SWIPT: Imperfect channel sensing," *IEEE Syst. J.*, vol. 12, no. 3, pp. 2361–2372, Sep. 2018.
[51] H. Q. Ngo, E. G. Larsson, and T. L. Marzetta, "Energy and spectral efficiency of very large multiuser MIMO systems," *IEEE Trans. Commun.*, vol. 61, no. 4, pp. 1436–1449, Apr. 2013.
[52] Y. Li, M. Sheng, X. Wang, Y. Zhang, and J. Wen, "Max-min energy-efficient power allocation in interference-limited wireless networks," *IEEE Trans. Veh. Technol.*, vol. 64, no. 9, pp. 4321–4326, Sep. 2015.

Chih-Lin Chuang received the B.S. degree in communication engineering from National Taipei University, Sanxia, Taiwan, in 2017, and the M.S. degree in electrical engineering from National Tsing Hua University, Hsinchu, Taiwan, in 2019.

His research interests include multiobjective evolutionary algorithms and wireless communication.

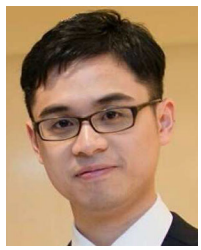

Wei-Yu Chiu (Member, IEEE) received the Ph.D. degree in communications engineering from National Tsing Hua University (NTHU), Hsinchu, Taiwan, in 2010.

He is currently an Associate Professor of electrical engineering with NTHU. His research interests include multiobjective optimization and reinforcement learning, and their applications to control systems, robotics, and smart energy systems.

Dr. Chiu was the recipient of the Youth Automatic Control Engineering Award bestowed by Chinese Automatic Control Society in 2016, the Outstanding Young Scholar Academic Award bestowed by Taiwan Association of Systems Science and Engineering in 2017, the Erasmus+ Programme Fellowship funded by European Union (staff mobility for teaching) in 2018, and the Outstanding Youth Electrical Engineer Award bestowed by the Chinese Institute of Electrical Engineering in 2020. From 2015 to 2018, he was an Organizer/Chair for the International Workshop on Integrating Communications, Control, and Computing Technologies for Smart Grid (ICT4SG). He is a Subject Editor for *IET Smart Grid*.

Yu-Chieh Chuang received the B.S. and M.S. degrees in electrical engineering under the supervision of Prof. Wei-Yu Chiu from National Tsing Hua University, Hsinchu, Taiwan, in 2018 and 2020, respectively.

His research interests include reinforcement learning and smart grids.